The Astrophysical Journal, 701:1732–1741, 2009 August 20 doi:10.1088/0004-637X/701/2/1732

THE FREQUENCY OF LOW-MASS EXOPLANETS

S. J. O'Toole[1,2], H. R. A. Jones[2], C. G. Tinney[3], R. P. Butler[4], G. W. Marcy[5,6], B. Carter[7], J. Bailey[3], and R. A. Wittenmyer[3]

[1] Anglo-Australian Observatory, P.O. Box 296, Epping 1710, Australia; otoole@aao.gov.au
[2] Centre for Astrophysics Research, University of Hertfordshire, Hatfield, AL 10 9AB, UK
[3] Department of Astrophysics, School of Physics, University of NSW, 2052, Australia
[4] Department of Terrestrial Magnetism, Carnegie Institution of Washington, 5241 Broad Branch Road NW, Washington DC 20015-1305, USA
[5] Department of Astronomy, University of California, Berkeley, CA 94720, USA
[6] Department of Physics and Astronomy, San Francisco State University, San Francisco, CA 94132, USA
[7] Faculty of Sciences, University of Southern Queensland, Toowoomba, Queensland 4350, Australia
Received 2008 November 17; accepted 2009 June 26; published 2009 August 4

ABSTRACT

We report first results from the Anglo-Australian Telescope Rocky Planet Search—an intensive, high-precision Doppler planet search targeting low-mass exoplanets in contiguous 48 night observing blocks. On this run, we targeted 24 bright, nearby and intrinsically stable Sun-like stars selected from the Anglo-Australian Planet Search's main sample. These observations have already detected one low-mass planet reported elsewhere (HD 16417b), and here we reconfirm the detection of HD 4308b. Further, we have Monte Carlo simulated data from this run on a star-by-star basis to produce robust detection constraints. These simulations demonstrate clear differences in the exoplanet detectability functions from star to star due to differences in sampling, data quality and intrinsic stellar stability. They reinforce the importance of star-by-star simulation when interpreting the data from Doppler planet searches. These simulations indicate that for some of our target stars we are sensitive to close-orbiting planets as small as a few Earth masses. The two low-mass planets present in our 24-star sample indicate that the exoplanet minimum mass function at low masses is likely to be a flat $\alpha \sim -1$ (for $dN/dM \propto M^{\alpha}$) and that between $15\% \pm 10\%$ (at $\alpha = -0.3$) and $48\% \pm 34\%$ (at $\alpha = -1.3$) of stars host planets with orbital periods of less than 16 days and minimum masses greater than 3 $M_{\oplus}$.

Key words: methods: numerical – methods: statistical – planetary systems – stars: individual (HD 4308, HD 16417, HD 84117)

Online-only material: color figures

1. INTRODUCTION

The planetary mass function is a key constraint which theories of star and planet formation must be able to accurately predict, if they are to be considered viable. While a consensus is emerging that planet formation, in general, is probably dominated by the growth of rocky cores via the accretion of dust particles and/or ices (i.e., the "core accretion" paradigm developed to explain the formation of the solar system, e.g., Pollack et al. 1996), the primary alternative scenario of direct gravitational collapse remains a plausible mechanism (e.g., Boss 2007).

Three indirect lines of reasoning suggest that terrestrial-mass planets could orbit at least a few percent of stars. The first planet with a minimum mass of less than 10 $M_{\oplus}$—GJ 876d—was identified just 3 yr ago. GJ 876d has a minimum ($m \sin i$) mass of 4.9 $M_{\oplus}$ and a probable mass of 7.5 $M_{\oplus}$ (Rivera et al. 2005). In the years since, a further five Doppler exoplanets have been announced with minimum masses of less than 10 $M_{\oplus}$ (Udry et al. 2007; Mayor et al. 2008). And a further two low-mass exoplanets have been revealed by gravitational microlensing searches (Beaulieu et al. 2006; Bennett et al. 2008). So there can be a little doubt that exoplanets below 10 $M_{\oplus}$ do indeed exist, though whether such planets are rocky ones (like the Earth) or icy ones (like Neptune and Uranus) is yet to be unambiguously demonstrated. Second, gas-giant planets exist around at least 6.5% of nearby main-sequence stars (Marcy et al. 2005a) and planet-formation theories suggest that rocky cores and embryos should accompany such Jovian planets (Wetherill & Stewart 1989; Goldreich et al. 2004; Kenyon & Bromley 2006). Finally, dusty protoplanetary disks are very common around young T Tauri stars, which suggests the ubiquity of the building blocks of rocky planets (Hillenbrand et al. 1998; Haisch et al. 2001; Mamajek et al. 2004).

While not definitive, these observations are suggestive of the existence of rocky planets outside our solar system. However, the theory of rocky planet formation remains less than solid. We do not know what fraction of stars forms rocky planets, nor how many of these planets avoid dynamical ejection by the larger planets. Worse, we do not know if rocky planets with masses above 1 $M_{\oplus}$ quickly accrete gas and volatile to become ice giants like Neptune and Uranus. This has been predicted by Ida & Lin (2004) and Goldreich et al. (2004), and would result in a planetary mass desert between 1 and 14 $M_{\oplus}$, as indeed we see in our solar system. This theory does suggest that disks with higher surface-mass density than the minimum-mass solar nebula are expected to produce numerous rocky planets formed closer to their parent star, which would make their Doppler detection more feasible (Ida & Lin 2004). Moreover, planets of 1–15 $M_{\oplus}$ may retain water in amounts that are comparable to the silicates and iron-peak elements, resulting in a family of ocean planets (Léger et al. 2004).

What is clear is that the detection of a statistically meaningful sample of planets between 5 $M_{\oplus}$ and 25 $M_{\oplus}$, along with measurements of their masses, radii, and orbits, will be required to significantly inform these diverse theories, and drive forward our detailed understanding of how planets form.

2. THE ANGLO-AUSTRALIAN PLANET SEARCH

The Anglo-Australian Planet Search (AAPS) is a long-term radial velocity program targeting the detection and parameterization of exoplanets. The AAPS' main survey targets 250 southern Sun-like stars, and has been in operation since 1998. To date the survey has discovered 32 new exoplanets orbiting stars in the main sample (Tinney et al. 2001, 2002a, 2003, 2005, 2006; Butler et al. 2001, 2002; Jones et al. 2002, 2003a, 2003b, 2006; Carter et al. 2003; McCarthy et al. 2004; O'Toole et al. 2007; Bailey et al. 2008). AAPS' precision Doppler measurements are made with the University College London Echelle Spectrograph (UCLES) echelle spectrometer (Diego et al. 1991). An iodine absorption cell provides wavelength calibration from 5000 to 6200 Å. The spectrograph point-spread function (PSF) and wavelength calibration are derived from the iodine absorption lines embedded on every pixel of the spectrum by the cell (Valenti et al. 1995; Butler et al. 1996). This observing and analysis system has demonstrated long-term precisions of 3 m s^{-1} for late-F, -G, and early-K dwarfs brighter than $V = 7.5$ (Tinney et al. 2005; Butler et al. 2001).

The UCLES dispersion through a 1″ slit gives an effective resolution of $\lambda/\Delta\lambda = 60000$. A precision of 1 m s^{-1} corresponds to displacements of 0.5 millipixel at our detector, and this, then, is the level below which we aim to hold the sum of all systematic uncertainties. Many subtle uncertainty issues enter at the level of 0.5 millipixel, such as determining the wavelength scale to nine significant digits, establishing the PSF shape at one part in 1000 (which varies dramatically with wavelength and seeing), measuring the charge transfer efficiency of the CCD, and calibrating the nonlinear response of the quantum efficiency of the CCD. In addition, we specifically treat the Earth's telluric H_2O and O_2 lines that contaminate our spectra at levels below 0.5% intensity, and we eliminate all ghosts and defects from the spectrometer and CCD, on a pixel-by-pixel basis. We also employ a fully relativistic Doppler correction to the barycenter of the solar system to remove the effect of the Earth's orbital motion and rotational spin.

Our data processing procedures follow those described by Butler et al. (1996, 2001, 2006) and Tinney et al. (2005). All data taken by the AAPS to date have been reprocessed through our continuously upgraded analysis system. The results presented in this paper arise from the current version of that pipeline.

3. THE ANGLO-AUSTRALIAN ROCKY PLANET SEARCH

The detection of very low-mass exoplanets by the AAPS and other Doppler programs within the last 4–5 yr has in large part been due to the dramatic improvements achieved in the measurement precisions of these searches. These have improved to such an extent that it is now clear that noise sources *intrinsic* to the parent star themselves are the limiting factor for a very low-mass exoplanet detection. The characterization of these noise sources (jitter, convective granulation, and asteroseismological *p*-mode oscillations) has become an important focus of Doppler planet detection. A few obvious modifications to current observing strategies have emerged: (1) target low-mass stars; (2) target chromospherically inactive and slowly rotating stars; (3) target high-gravity stars (where *p*-mode oscillations are minimized); and (4) extend the observations of stars over several *p*-mode fundamental periods, so that asteroseismological noise is averaged over.

The Anglo-Australian Rocky Planet Search specifically seeks to focus on the last three of these observing strategies in an effort to push to the lowest possible detection limits achievable with our system. That is, it focuses on the observation of bright stars known to be relatively stable to radial velocity jitter (e.g., Wright 2005). We ensure that all observations of each target are of sufficient length to average over the dominant asteroseismological period for each target star. For this purpose, we employed the algorithms of O'Toole et al. (2008) to derive the maximum asteroseismological beat period ($P_{\rm max}$) for each star, and then ensure that observations are *at least* this long. Observations of our Rocky Planet Search targets, which typically spanned 15–20 minutes, easily achieved this goal.

Finally, and most importantly, observations are carried out over long, contiguous observing runs of 48 nights. These long observing blocks are critical as they allow us to integrate up Fourier power and suppress sidebands in the window function over many periods. The first of these Rocky Planet Search observing blocks was scheduled on the 3.9 m Anglo-Australian Telescope (AAT) from 2007 January 10 to 2007 February 26, spanning two full bright lunations and the dark and gray time in between.

The power of this intensive observing approach is most simply and dramatically demonstrated by our detection of the short-period planet HD 16417b (O'Toole et al. 2009a) from 24 epochs obtained on that run, and the *non-detection* of the same planet in a similar quantity of similar quality data spread over a 2 yr period. This bears out the simulations performed by other investigators—that to detect planets with amplitudes of 1–3 times that of the net measurement uncertainty, it is necessary to acquire observations over many contiguous periods (see, for example, Narayan et al. 2005).

3.1. Sample Selection

The stars chosen for Rocky Planet Search observation on this first run were a subset of the AAPS main sample (Jones et al. 2003a) that are bright ($V < 6.7$), inactive ($\log R'_{\rm HK} < -4.8$) and in the right ascension range 0–17$^{\rm h}$ with southerly declinations, suitable for observation in January and February at the AAT. All the stars in the sample had asteroseismological period, $P_{\rm max}$, less than 800 s. It includes 24 F, G, and K stars. No metallicity criteria were used in this selection. Stars with known stellar companions within 2″ are removed from the observing list as it is operationally difficult to get an uncontaminated spectrum of a star with a nearby companion. One star which satisfied these criteria (HD 75289) has a known exoplanet in 3$^{\rm d}$.5 orbit (Udry et al. 2000; Butler et al. 2006) of such high-amplitude ($K = 54$ m s^{-1}) that it would have significantly complicated the possibility of detecting a low-mass planet. As a result, it was not included in the observed sample. Otherwise, stars were not rejected on the basis of having known exoplanets. HD 4308 was selected for inclusion in this sample when the observing program was first proposed in 2005, and was retained for observation even after a low-amplitude planet ($K = 4$ m s^{-1}) was announced in a 15$^{\rm d}$.1 orbit by Udry et al. (2006).

The stars observed, and their properties, are summarized in Table 1. All of these stars have been included in large-scale studies of nearby solar-type stars. Nordström et al. (2004) included them in a magnitude-limited, kinematically unbiased study of 16,682 nearby F and G dwarf stars. Valenti & Fischer (2005) included them in a study of the stellar properties for 1040 F, G and K stars observed for the Anglo-Australian, Lick and Keck planet search programs. Valenti & Fischer used high signal-to-noise ratio (S/N) echelle spectra (originally taken as radial velocity template spectra) and spectral synthesis to derive effec-

Table 1
Stellar Parameters for Twenty Four Rocky Planet Search Targets

HD	R.A.	Decl.	V (mag)	SpTyp	$\log R'_{HK}$	P_{max} (s)	[Fe/H]		$v \sin i$ (km s^{-1})	Age (Gyr)		Mass ($M_\odot$)	
							VF05	N04		VF05	N04	VF05	N04
1581	00 20 04.2	−64 52 29	4.23	F9.5V	−4.92	314	−0.22	−0.18	3.0	5.3	8.2	1.00	0.97
4308	00 44 39.2	−65 38 58	6.55	G5V	−5.07	234	−0.31	−0.34	0.2	9.5	17.1	0.91	0.85
10361	01 39 47.2	−56 11 44	5.81	K5V	−4.88	216	−0.22	−0.17	1.9	4.5	...	0.77	0.78
10360	01 39 47.7	−56 11 34	5.87	K0V	−4.95	207	−0.23	−0.16	2.2	5.5	...	0.75	0.79
10700	01 44 04.0	−15 56 15	3.50	G8V	−4.94	214	−0.52	−0.42	1.3	...	...	0.97	0.81
16417	02 36 58.6	−34 34 41	5.79	G5IV	−5.08	614	+0.13	+0.01	2.1	5.8	7.6	1.18	1.1
20794	03 19 55.6	−43 04 11	4.27	G8V	−4.98	333	−0.41	−0.30	1.5	13.5	8.3	0.82	0.83
23249	03 43 14.9	−09 45 55	3.52	K0V	−5.18	883	+0.16	...	2.6	6.6	...	1.19	...
26965	04 15 17.6	−07 38 40	4.43	K1V	−4.87	260	−0.28	−0.05	0.5	12.2	16.9	0.78	0.84
28255A	04 24 12.2	−57 04 17	6.29	G4V	−4.85	250	+0.05	+0.08	2.7	2.8	9.1	1.07	1.05
43834	06 10 14.4	−74 45 11	5.09	G6V	−4.94	311	+0.09	+0.10	1.7	5.4	12.8	0.98	0.91
53705	07 03 57.3	−43 36 29	5.54	G3V	−4.93	324	−0.21	−0.32	1.6	7.2	12.9	0.97	0.81
72673	08 32 52.2	−31 30 10	6.38	K0V	−4.89	229	−0.37	−0.47	0.0	8.1	...	0.78	0.77
73524	08 37 19.9	−40 08 52	6.53	G4IV–V	−4.96	388	+0.12	−0.02	3.1	3.1	7.0	1.14	1.03
84117	09 42 14.4	−23 54 56	4.93	G0V	−4.97	452	−0.07	−0.14	5.7	3.1	4.6	1.15	1.09
100623	11 34 29.9	−32 50 00	5.96	K0V	−5.07	221	−0.37	−0.51	0.7	7.8	...	0.77	0.76
102365	11 46 31.0	−40 30 01	4.91	G5V	−4.95	344	−0.33	−0.29	0.7	11.0	16.1	0.86	0.86
114613	13 12 03.1	−37 48 11	4.85	G3V	−5.03	727	+0.24	...	2.4	4.9	...	1.28	
115617	13 18 24.9	−18 18 31	4.74	G5V	−4.95	314	+0.05	+0.04	2.2	6.3	12.3	0.95	0.89
122862	14 08 27.1	−74 51 01	6.02	G2.5IV	−4.99	680	−0.13	−0.36	2.6	5.9	8.4	1.13	1.02
128621	14 39 35.0	−60 50 14	1.33	K1V	−4.92	245	+0.23	+0.15	0.9	8.0	...	0.89	...
128620	14 39 36.4	−60 50 02	−0.0	G2V	...	415	+0.21	+0.15	2.3	4.3	...	1.12	...
136352	15 21 48.1	−48 19 03	5.65	G4V	−4.91	397	−0.34	−0.32	2.0	10.9	15.9	0.89	0.85
146233	16 15 37.1	−08 22 06	5.49	G1V	−5.05	336	+0.03	+0.03	2.6	4.7	8.3	1.02	0.98

Notes. Coordinates and magnitudes are based on the Hipparcos catalog (Perryman et al. 1997); spectral types are from Houk (1982); activities are from Henry et al. (1996); Tinney et al. (2002b); Jenkins et al. (2006); metallicities, isochrone masses, and ages are from Valenti & Fischer (2005, VF05) and Nordström et al. (2004, N04).

tive temperatures, surface gravities, and metallicities, whereas Nordström et al. (2004) used Strömgren photometry and the infrared flux calibration of Alonso et al. (1996). Both studies use Hipparcos parallaxes to obtain luminosities and make comparisons with different theoretical isochrones to derive stellar parameters. To determine stellar masses and ages Valenti & Fischer use Yonsei–Yale isochrones (Demarque et al. 2004), while Nordström et al. (2004) use Padova isochrones (Girardi et al. 2000; Salasnich et al. 2000). Both sets of derived parameters are consistent to within the uncertainties of these studies.

3.2. Observations

The observing strategy on each night was straightforward—to observe every star in the target list for at least 15 min (or as long as is required to obtain S/N ≈ 400 per spectral pixel given the available transparency and seeing conditions) on each of the 48 nights of observing. The number of observations actually obtained for each of the 24 targets is given in Table 2 and ranges from 18 to 44, with a median of 31. The second column in this table provides the rms for each target about the mean velocity, with four exceptions—the values given for the two stars with planets (HD 16417 and HD 4308—see below) are the rms of the residuals after a best-fit planet was subtracted, and the values for the two components of the binary system α Cen (HD 128620 and HD 128621) have had linear trends subtracted. The "Act. jitter" column shows the activity jitter derived using an updated version (J. T. Wright, private communication) of the Wright (2005) recipe, which is considered to produce jitter estimates good to ±50%. The "Osc. jitter" column gives the oscillation jitter (from O'Toole et al. 2008) for the average exposure time used for each target. To present these results graphically, histograms of the measured Doppler velocities are shown in Figure 1 for each object (with the plots for HD 4308, HD 16417, HD 128620, and HD 128621 showing residuals as described above). Overplotted are Gaussians with full width at half-maximum (FWHM) equal to the rms (dashed line) and the activity jitter (dotted line) for each object.

There is at least one case (HD 84117) where the observed velocity variability distribution appears to deviate significantly from a Gaussian distribution. We therefore plot the actual velocities obtained for this object in Figure 2, which show evidence for significant variability over the course of the 48n run, though with no obvious periodicity, nor with an obviously Keplerian shape. (No other star observed on this run shows a similar variability trend, indicating that the variability seen is not a systematic effect of our measurement system.) Adding in additional AAPS data of similar quality taken since 2005 January 30 indicates that HD 84117 has shown excess velocity variability since 2005 over that expected from activity jitter alone (with an rms of 4.7 m s^{-1}). The periodogram of HD 84117 shows essentially no power at periods of less than 40 d, though a complex, broad power distribution is seen at longer periods, i.e., longer than the time span of the observations. We can therefore fit the data with no compelling single Keplerian. HD 84117 may either contain multiple planets, which will require intensive observation to disentangle, or may be a star with an unusual class of velocity variability. We can nonetheless say with confidence that it does not host a low-mass exoplanet in an orbit of less than ∼30 d.

Thirteen of the 24 stars have observed rms values consistent with their jitter estimates to within ±50%, and all but

Table 2
Rocky Planet Search Observations

Target	N_{obs}	rms ($m\ s^{-1}$)	Median Unc. ($m\ s^{-1}$)	Act. Jitter ($m\ s^{-1}$)	Osc. Jitter ($m\ s^{-1}$)
1581	24	1.90	0.65	4.44	0.20
4308	24	2.24	1.09	2.17	0.12
10,360	22	4.09	0.83	2.10	0.04
10,361	18	3.79	0.77	2.10	0.04
10,700	24	1.80	0.57	2.10	0.10
16,417	24	1.57	0.78	2.19	0.35
20,794	28	3.06	0.52	1.80	0.12
23,249	27	1.94	0.34	4.85	0.43
26,965	28	3.22	0.55	1.80	0.07
28,255A	28	6.12	1.10	6.20	0.08
43,834	37	3.07	0.61	1.80	0.12
53,705	44	3.02	1.02	2.10	0.16
72,673	42	2.51	0.98	1.80	0.07
73,524	33	4.34	1.10	2.58	0.14
84,117	37	5.43	1.11	3.00	0.23
100,623	34	2.87	0.94	2.10	0.05
102,365	39	2.21	0.74	2.10	0.14
114,613	37	3.66	0.57	3.42	0.45
115,617	41	3.92	0.61	1.80	0.14
122,862	31	3.60	1.10	2.70	0.34
128,620	20	1.06	0.25	1.80	0.23
128,621	31	2.28	0.40	1.80	0.12
136,352	32	4.02	1.09	2.10	0.17
146,233	23	3.21	0.88	2.19	0.16

Notes. N_{obs} indicates the number of nights on which the object was observed. An observation on any particular night always comprises at least three separate exposures. Also given is the velocity scatter (rms), median velocity uncertainty, activity jitter (see the text), and oscillation jitter (from O'Toole et al. 2008). The latter is based on the average exposure time for each target and is given as a guide.

two are consistent to within a factor of 2—this is in line with expectations if the jitter estimates have a 1σ uncertainty of $\pm 50\%$. The two outliers in this comparison are HD 1581 (F9.5V) and HD 23429 (K0V), where the observed velocity variation is much less than that predicted by the jitter model (by factors of 2.3 and 2.5, respectively), and HD 115617 (G5V) where the level of variability observed is larger than that predicted by the jitter model (by a factor of 2.2). The activity jitter estimate does not include velocity variability due to asteroseismological oscillations (which is in general much smaller than the activity jitter—see Table 2) and more importantly, does not include the effects of convective granulation, which is (to date) unparameterized for any Doppler planet search stars. What can be concluded is that at very high velocity precisions, even "inactive" stars remain velocity variable at low levels.

3.3. Planets in the Sample

There are two objects in our target list that have detectable planets orbiting them: HD 4308 and HD 16417. The latter was discovered as a part of this observing campaign with $P = 17.24 \pm 0.^{d}01$, $e = 0.20 \pm 0.09$, and $m \sin i = 22.1 \pm 2.0\ M_{\oplus}$. It is presented in a separate paper (O'Toole et al. 2009a) to which we refer the reader for further details.

HD 4308b was discovered by Udry et al. (2006) and is a $\sim 13\ M_{\oplus}$ planet in a $15.^{d}6$ orbit around a G5 dwarf. It was observed 25 times during our campaign and the $15.^{d}6$ period is clearly evident in the two-dimensional Keplerian Lomb–Scargle (2DKLS) periodogram (O'Toole et al. 2007) shown in Figure 3. The data from this run alone are indeed sufficient to a Keplerian fit which measures similar orbital parameters (see Figure 4) to the Udry et al. data. A scrambled velocities false-alarm-probability test (FAP—Marcy et al. 2005a) indicates that for 5000 trials, $\sim$16% of scrambled velocities for this data set give a reduced chi-squared better than the solution.

To refine the orbital parameters of HD 4308b, we have combined the velocities published in Udry et al. (2006) with our AAPS velocities—this includes both the observations obtained of HD 4308 in the Rocky Planet Search run of 2007 January–February, and other AAPS observations obtained with a similar S/N between 2005 October 21 and 2007 November 27. These observations are listed in Table 3. The 2DKLS periodogram based on this combined data set is shown in Figure 5. The inset in this figure shows the corresponding slice through the 2DKLS at a constant period, as a function of eccentricity, and demonstrates how eccentricity is not well constrained by this data set.

In Figure 4, we show our best fit to the HD4308 data from the Rocky Planet Search run alone, while in Figure 6 we show the combination of all high-S/N data from the AAT and published HARPS data, and list the derived parameters in Table 4. (The mass for HD 4308 of $0.91 \pm 0.05\ M_{\odot}$ due to Valenti & Fischer (2005) is adopted, as is a jitter estimate for HD 4308 of 2.17 $m\ s^{-1}$.) We have determine a FAP for this planet of $<0.02\%$, based again on 5000 scrambled velocity data sets. Though the eccentricity derived from the combined data set ($e = 0.27 \pm 0.12$) is higher than that published by Udry et al., we note two points in relation to this: first that it has been recently demonstrated by several studies (O'Toole et al. 2009b; Shen & Turner 2008) that there is a systematic bias against measuring zero eccentricities for low-amplitude planets; and second that the uncertainty estimates for eccentricity produced by the least-squares fit of Keplerians can seriously underestimate the true eccentricity's uncertainty represented by a data set (O'Toole et al. 2009b). Given this, we do not believe that the differences between the Keplerian parameters for HD 4308b derived here and by Udry et al. are significant.

Finally, we note that the residuals to the Rocky Planet Search data alone (Figure 4) are suggestive of a further periodicity in that data set at 30–40 d. To examine the possibility of there being a second planet present in these data, we have constructed the 2DKLS for the AAT and HARPS velocities with the Keplerian of Figure 6 removed (see Figure 7). The result is suggestive of power at periods between 30 d and 80 d. While potential planets at 32 d and 48 d periods can be fitted to these data, they do not do so with a significance that warrants a claim to have detected further planets in this system.

4. SIMULATIONS

The biases inherent in planet search observing and analysis strategies remain the largest single hurdle to a robust understanding of the formation processes that have built the 300-odd exoplanets known to date. Considerable work has been conducted on trying to eliminate these underlying biases from Doppler exoplanetary statistics (e.g., O'Toole et al. 2009b; Wittenmyer et al. 2006; Cumming et al. 1999, 2003, 2008; Cumming 2004).

To assess the selection functions delivered by the AAPS, we work toward a detailed understanding of Doppler noise sources intrinsic to stars (e.g., O'Toole et al. 2008). We then use detailed object-by-object Monte Carlo simulations (O'Toole et al. 2009b) to explore the biases introduced by these noise sources, when combined with our observational window functions.

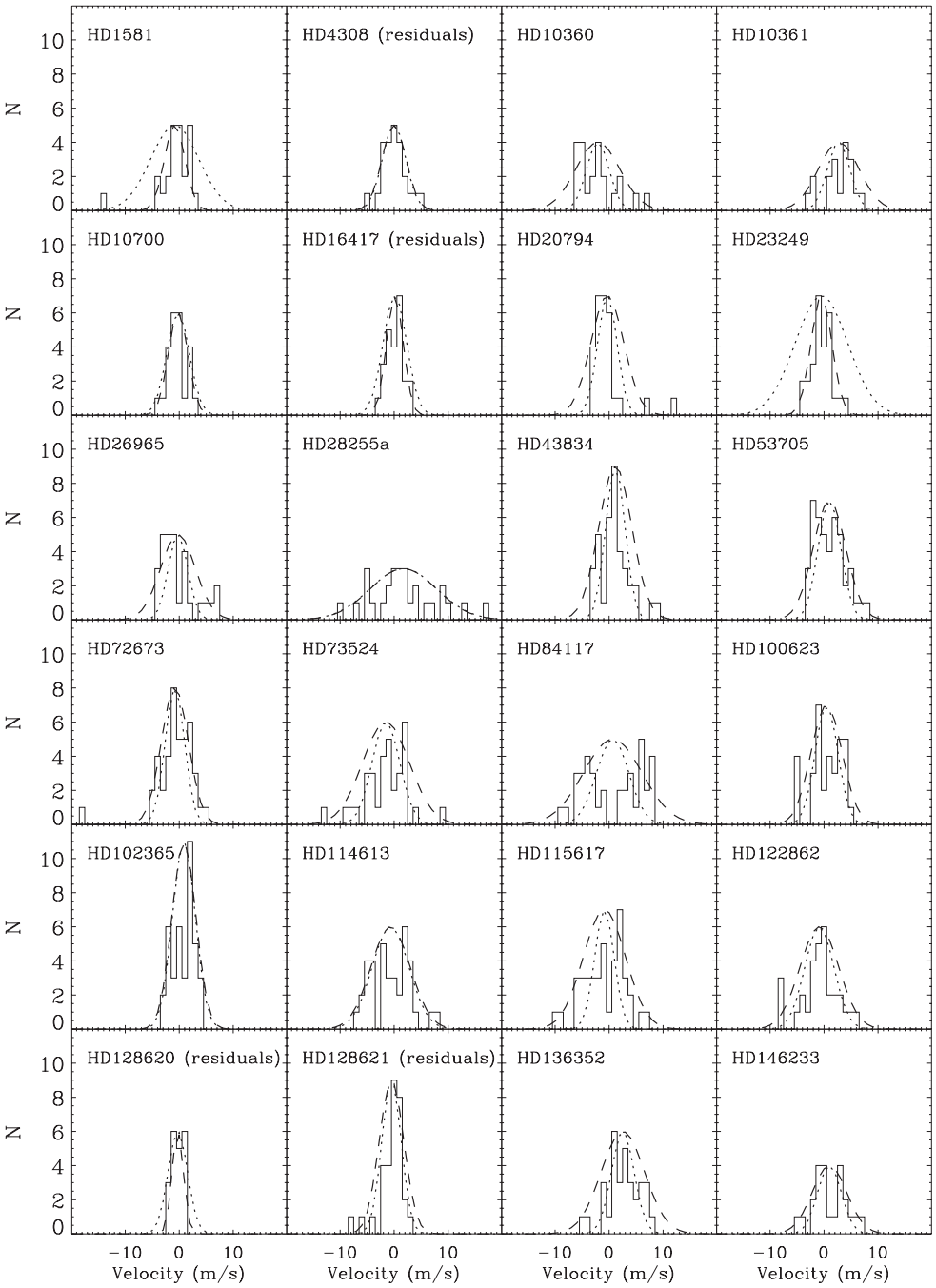

Figure 1. Histograms of measured Doppler velocities for each of our 24 targets. Also plotted are Gaussians with the FWHM equal to the stellar jitter (dotted) and the velocity scatter (dashed). Histograms of the residuals are shown for the two objects with known planets (HD 4308 and HD 16417), while the binary system α Cen (HD 128620 and HD 128621) have had a linear trend subtracted.

The procedure we employ is to generate single Keplerians for a grid of periods, eccentricities, and semi-amplitudes, which are then sampled at the actual observation time stamps and which have noise added to them in line with the actual measurement uncertainties and stellar noise appropriate for each epoch. These simulated observations are then subjected to an automated detection process, enabling us to determine the range of period, planet mass, and orbital eccentricity to which each data set is sensitive. The simulations are performed using the Keter and Swinburne supercomputer facilities. Details of the simulations and detectability criteria are described in O'Toole et al. (2009b), though with the modification to the procedure in that paper (which describes the analysis of purely artificial data), that the simulations of *actual* data, used here, include added noise terms due to intrinsic stellar velocity variability (Wright 2005; O'Toole et al. 2008).

To simulate the 48 nights data obtained on this first Rocky Planet Search run, we used a subset of the model grid from O'Toole et al. (2009b) with input periods on a logarithmic scale from $\log_{10} P = 0.3, 0.6, 0.9, 1.2$ (i.e., periods between 2 d and 16 d); input eccentricities of 0.0, 0.1, and 0.2; and planet masses of 0.01, 0.02, 0.05, 0.1, 0.2, and 0.5 $M_{\rm Jup}$. The eccentricity range simulated was deliberately limited to the "near-circular" range of $e = 0.0$–0.2, since (a) the majority of planets in such small orbits (i.e., <0.12 ÅU) will have undergone significant tidal circularization, and (b) the vast majority of detected Doppler

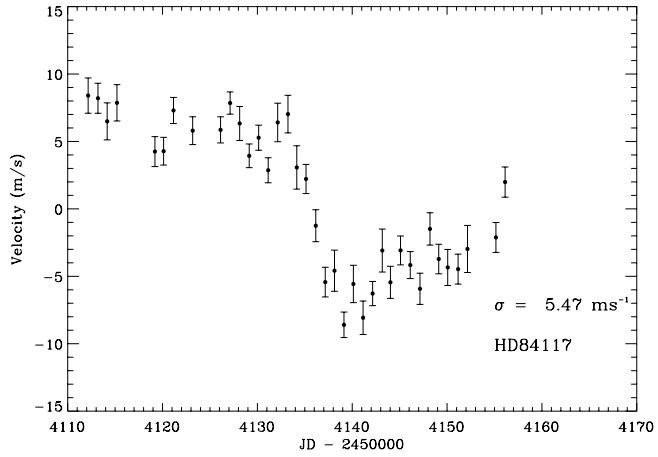

Figure 2. Data from the Rocky Planet Search run for HD 84117.

Table 3
AAT Doppler Velocities for HD 4308

JD (−2450, 000)	Velocity (m s^{-1})	JD (−2450, 000)	Velocity (m s^{-1})
3665.119898	−0.3 ± 0.9	4120.935790	−2.4 ± 1.7
3666.110456	−0.6 ± 0.9	4125.954730	1.7 ± 1.1
3668.136398	2.8 ± 0.8	4126.924257	2.6 ± 1.2
3669.119458	0.6 ± 0.9	4127.931946	3.7 ± 1.1
3670.126654	4.5 ± 1.1	4128.927984	0.5 ± 1.0
3671.147771	3.6 ± 1.3	4129.930445	1.1 ± 1.0
3698.032791	−9.0 ± 1.0	4130.924765	−0.1 ± 0.9
3700.063296	−0.7 ± 0.8	4131.937199	−0.2 ± 1.1
3702.062004	1.1 ± 1.3	4133.927357	−2.3 ± 0.9
3938.327905	5.9 ± 1.0	4134.931174	0.5 ± 1.0
3942.284604	−0.1 ± 0.9	4135.948345	−1.5 ± 0.9
3943.328172	2.6 ± 0.8	4136.945095	3.1 ± 1.0
3944.283860	−1.3 ± 0.9	4137.977861	6.6 ± 1.3
3945.320288	−3.8 ± 0.9	4140.931894	7.5 ± 1.3
3946.318428	−4.6 ± 0.9	4145.918589	5.0 ± 1.2
3947.328379	−5.5 ± 1.0	4149.900027	−4.6 ± 1.1
4008.152191	−1.1 ± 1.0	4153.907836	1.6 ± 1.1
4009.177898	−0.0 ± 1.0	4154.918636	4.5 ± 1.2
4010.168991	0.2 ± 0.9	4253.327811	0.4 ± 0.9
4011.141538	−2.4 ± 0.9	4255.246671	−3.1 ± 1.3
4012.129794	−2.5 ± 0.9	4256.321705	−2.6 ± 1.2
4013.171260	−0.2 ± 0.9	4257.304964	−3.6 ± 1.7
4014.188894	−2.6 ± 1.2	4334.157294	3.0 ± 1.2
4016.210211	−1.5 ± 1.0	4335.254660	7.8 ± 2.7
4018.142500	−0.1 ± 1.0	4336.264333	−3.7 ± 1.3
4037.046606	8.5 ± 0.8	4338.306202	−8.4 ± 1.4
4038.125336	4.6 ± 1.0	4369.133832	−0.3 ± 0.9
4039.054689	0.4 ± 1.0	4371.241454	−1.5 ± 1.0
4040.053384	−2.3 ± 0.9	4372.138956	5.5 ± 1.2
4041.068042	−0.4 ± 0.8	4373.185170	2.7 ± 1.3
4111.941520	3.1 ± 1.2	4375.180751	0.6 ± 1.0
4112.942694	4.1 ± 1.1	4425.078066	0.2 ± 1.1
4113.949634	0.3 ± 1.7	4429.012543	−2.0 ± 1.1
4114.947273	−0.4 ± 1.0	4429.946086	−4.9 ± 0.9
4118.926666	−8.9 ± 1.1	4431.004964	−6.9 ± 1.2
4119.920872	−6.7 ± 1.1	4431.997618	−5.8 ± 1.2

Notes. Julian Dates (JD) are heliocentric. Velocities are barycentric but have an arbitrary zero point.

exoplanets with periods of less than 16 d have eccentricities, $e < 0.2$ (e.g., Marcy et al. 2005b). As our data are approximately evenly sampled (each star was observed on average once per night at approximately the same time), we have supplemented the above with additional simulations at the same eccentricities

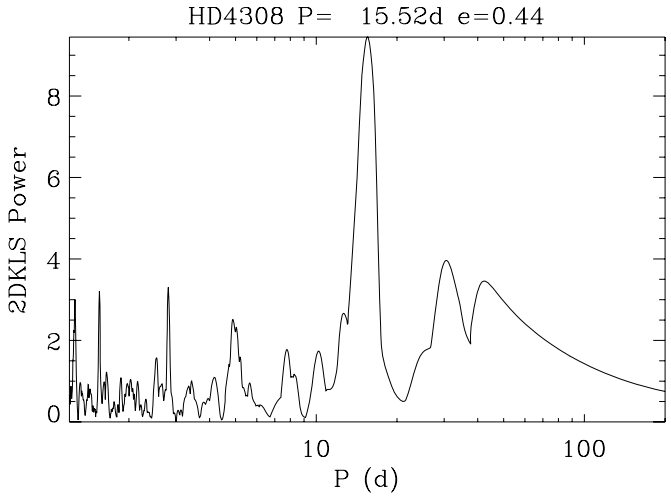

Figure 3. 2DKLS Periodogram evaluated at $e = 0.44$ determined for HD 4308 from AAT Rocky Planet Search data alone.

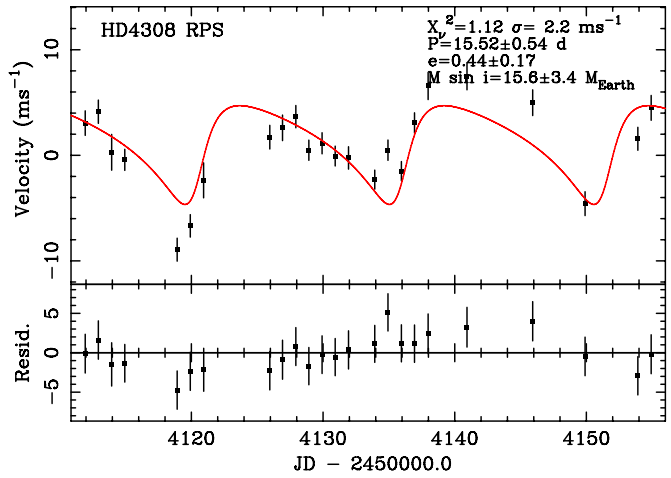

Figure 4. Keplerian fit to HD 4308 data from the Rocky Planet Search (RPS) run.

(A color version of this figure is available in the online journal.)

and masses, but with non-integer periods of 2.8, 4.3, 5.6, 8.7, 11.2, 17.4, and 22.4 days. Because the Keplerian function of a Doppler exoplanet is unable to determine the inclination angle to the line of sight, i, no attempt has been made to deal with this in these simulations. As a result, whenever we refer to "mass" for a simulated planet in the following discussion, we are actually probing the $m \sin i$ "minimum mass" of that planet. For each (period, eccentricity, planet mass) point in this grid, 100 realizations are performed each with random noise added appropriate to the combined impact of the uncertainty at that time stamp and the jitter and p-mode noise appropriate for that star (see Table 2). Each star, then, is the subject of 21,600 simulations.

These simulations allow us to generate estimates of the detectability, for each star, of putative planets at each (mass, period, eccentricity) point in the simulations. In this context, we define "detectability" at a given set of orbital parameters as the number of detections (using the detection criteria of O'Toole et al. 2009b) divided by the corresponding total number of realizations. We have then integrated this detectability over eccentricity, since (a) detectability is approximately constant with eccentricity at the values we have simulated (see O'Toole

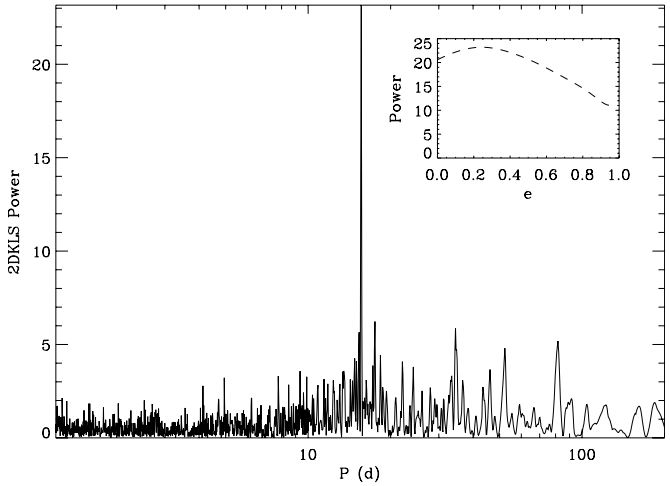

Figure 5. 2DKLS periodogram determined at $e = 0.24$ for HD 4308 from AAT data (2005 October–2007 November, including Rocky Planet Search data) and HARPS data (Udry et al. 2006). The inset shows 2DKLS power as a function of eccentricity at constant period and demonstrates how weakly this data set (in common with most Doppler data sets) constrains eccentricity.

Table 4
Orbital Parameters for HD 4308b

Parameter	AAT & HARPS	HARPS
Orbital period P (days)	15.609 ± 0.007	15.56 ± 0.02
Semi-amplitude K (m s^{-1})	3.6 ± 0.3	4.07 ± 0.2
Eccentricity e	0.27 ± 0.12	0.00 ± 0.01
Periastron (JD−2450000)	108.5 ± 1.9	3314.7 ± 2.0
ω (°)	210 ± 21	359 ± 47
$m \sin i$ ($M_\oplus$)	13.0 ± 1.4	15.1 ± 0.5[a]
Semi-major axis (AU)	0.118 ± 0.009	0.119 ± 0.009[a]
N_{fit}	113	41
rms (m s^{-1})	2.6	1.3
χ^2_ν	1.17	1.3

Notes.
[a] $m \sin i$ and semi-major axis numbers are those derived from the kinematic parameters of Udry et al. (2006), but assuming the same host-star mass (0.91 ± 0.05 $M_\odot$) used in this paper.

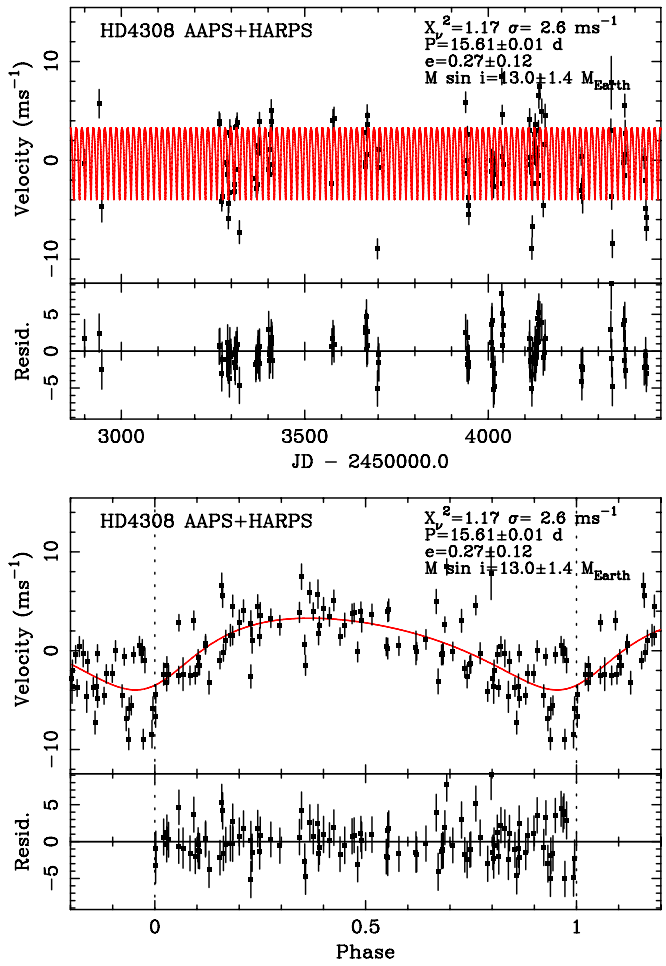

Figure 6. Velocities for HD 4308 from the AAT (2005 October–2007 November, including Rocky Planet Search data) and HARPS (Udry et al. 2006) plotted against time (upper panel) and phased at the best-fit orbital period (lower panel). The line indicates the best-fit Keplerian to this combined data set, the parameters of which are listed in Table 4.

(A color version of this figure is available in the online journal.)

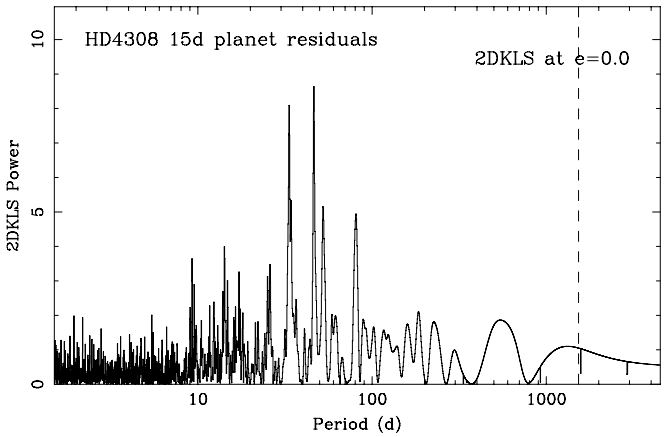

Figure 7. 2DKLS at $e = 0.0$ for the HD 4308 velocities of Table 3 after removal of the best-fit Keplerian of Figure 6. While there is some evidence for excess power at 30–80 d periods, this is not currently sufficient to justify claiming the detection of a second planet. (The vertical dashed line indicates the time span of the observations used to make this periodogram.)

et al. 2009), and (b) we wish to focus on our survey's sensitivity to the planet mass and period. The result is a set of surfaces indicating detectability as a function of $m \sin i$ and the period. These surfaces are shown in Figure 8 for two examples (HD 4308 and HD 53705), as well as for the whole sample of 24 objects.

The specific examples shown for HD 4308 and HD 53705 display the general features seen in the simulations of all the targets: first that detectability is very high at periods longer than a few days and at masses above 20 $M_\oplus$; and second that the details of the detectability contours vary from object to object. The primary cause for this is the different time and S/N sampling of the observations of each star. This reinforces the importance of simulating radial-velocity data on a star-by-star basis, rather than on a survey sensitivity basis. We note that the structure in the surfaces at ∼2 and ∼4 days is an effect of sampling; the observations were taken on average once per night at approximately the same time. This means that planets with periods that are integer multiples of this have poorly constrained parameters and are therefore harder to detect.

And finally, we must ask how many planets are detected from our actual observations if we apply to them the same automated criteria used to detect planets from the simulated data sets? Reassuringly, we find that just two planets are detected (HD 4308b and HD 16417b, although the former is perhaps marginal)—none of the other stars reveal planets that pass our automated detection criteria.

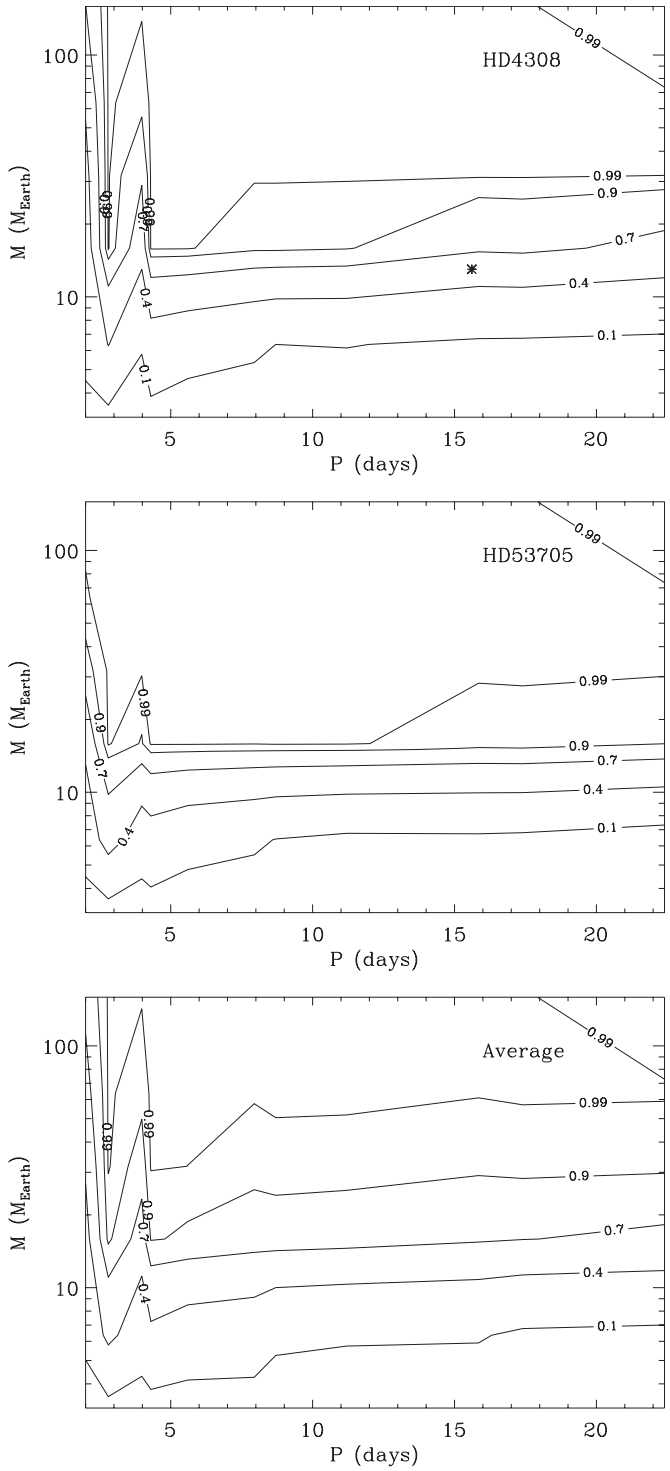

Figure 8. Detectability contours for planets as a function of input period and input planet mass (i.e., Doppler $m \sin i$ minimum mass) for two example stars (HD 4308 and HD 53705), and averaged over all 24 stars. (See the text for our formal definition of "detectability.") The known exoplanet HD 4308b is shown as an asterisk. The data for HD 4308 allow us to recover the previously detected planet—in comparison the HD 53705 data demonstrate significantly larger sensitivity to lower mass planets, due to the better sampling that was achieved on this run for this star. Averaged over the whole sample, the 10% detectability contour extends down to 3 $M_\oplus$ for periods from 2–10 d.

5. DISCUSSION

We can see from the average detectability surface in Figure 8 that the sensitivity of our survey of these 24 stars extends down to detectabilities of 10% or more at masses of 5 $M_\oplus$ over periods of 2–10 d. For higher mass planets, the survey is more sensitive, with the detectability being 40% or better for all planets with minimum mass >14 $M_\oplus$ and period >3 d.

With two planets known with minimum masses of 13.0 and 22.1 $M_\oplus$ from a survey of 24 stars, the first-order conclusion that can be drawn from this data set is that for periods of 2–16 d the frequency of low-mass (i.e., $m \sin i = 10 - 25 M_\oplus$) planets is $\sim 8\% \pm 6\%$. However, this neglects both the fact that we know that our detectability is less than perfect (though nonzero) over this mass range, and the fact that we know that our planet detectability is a strong function of planet mass and a weak function of the planet period. These effects need to be accounted for if we are to draw more robust conclusions from this survey.

For different exoplanet mass functions, we would expect our survey to have sensitivity to different masses. Put simply, a very steep exoplanet mass function should counteract our detectability surfaces to enable the detection of planets in the very lowest masses. Conversely, a flatter mass function should bias our results toward the detection of higher mass planets. So we should be able to use our data and simulations to provide much more insight into the frequency of low-mass planets.

If we parameterize the planet mass function as a power-law $dN/dM \propto M^\alpha$ (we assume for simplicity that there is no change in the incidence of planets over this period range at these masses), we can ask, given our known detectability surface as a function of the mass and period, what normalization of that power law would give us two exoplanet detections from our survey. Given our assumption that planet frequency is independent of the period in this period range, and because detectability is also a weak function of the period in this range, we make further simplifying assumption that we can integrate over the detectability surface at a given mass to derive an average detectability as a function of mass alone $D_P(M)$.

We can then write the number of planets detected from our survey, $N_{\rm Det}$, as a function of the number of stars observed $N_{\rm stars}$, the average frequency of planets in a given mass and the period range, F, the detectability as a function of mass, $D_P(M)$, and the power-law mass function,

$$N_{\rm Det} = F \times N_{\rm stars} \times \int D_P(M) \times M^\alpha \, dM$$

from which (given $N_{\rm Det} = 2$) we can derive F (averaged over the period range P = 2–22 d and the mass range[8] 0.01–20 $M_{\rm Jup}$), which varies from 0.14 ± 0.10 at $\alpha = -0.25$, up to 0.70 ± 0.85 at $\alpha = -1.75$, in the F, G, and K stars probed here. These planet frequencies might seem high in comparison to other work, though this is almost certainly due to the much lower masses being considered. For example, in Figure 12 of Cumming et al. (2008), these authors find an exoplanet frequency of 3% for periods less than 16 days and masses above 30 $M_\oplus$. The data presented here, in comparison, include significant sensitivity down to 4 $M_\oplus$. The normalizations found here are, of course, uncertain due to the Poisson-counting statistics of just two detections (in a sample of 24 stars), and do only probe a relatively small range of periods (or equivalently, semi-major axes). Having said that, this survey is important in being one of the first Doppler surveys of low-mass exoplanets with robustly characterized selection effects.

[8] Detectability has been extrapolated to the masses in this range higher than those that were simulated; however, this contributes a negligible uncertainty as the detectabilities for these more massive mass planets are very close to 1.0.

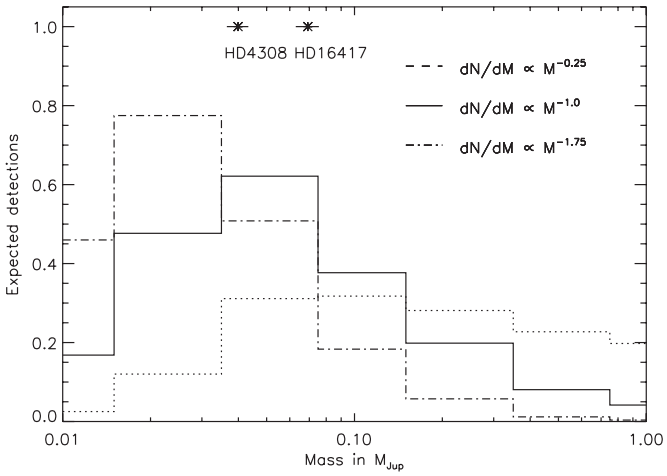

Figure 9. Expected number of exoplanet detections in our survey of 24 stars for different mass functions. The asterisks with uncertainties indicate the exoplanets HD 16417b and HD 4308b with $m \sin i$ masses of 0.0692 and 0.0442 $M_{\rm Jup}$, respectively.

Figure 9 shows how the expected number of detected planets varies as a function of different underlying mass functions (along with the $m \sin i$ minimum masses for the two detected planets in this survey, HD 4308b and HD 16417b). As expected, a different peak in the expected number of *observed* exoplanets is predicted for different mass functions. $\alpha = -1.75$ leads to a peak in the number of detected planets around 0.02 $M_{\rm Jup}$ (6.3 $M_\oplus$), the $\alpha = -1.0$ expected detections peak at around 0.05 $M_{\rm Jup}$ (16 $M_\oplus$), while the flatter $\alpha = -0.25$ mass function produces an expected detection peak at around 0.10 $M_{\rm Jup}$ (32 $M_\oplus$).

Given that we have found two exoplanet signals in the 16–25 $M_\oplus$ minimum mass range (corresponding to the 0.05 $M_{\rm Jup}$ or 16 $M_\oplus$ bin in Figure 9), we may consider these as providing the first available rough limits on the underlying mass function as determined by how changes in the mass function cause the peak of detections to move toward and away from the 0.05 $M_{\rm Jup}$ (16 $M_\oplus$) bin. We find that the peak moves from the 0.02 to the 0.05 $M_{\rm Jup}$ bin for α values shallower than $\alpha = -1.3$ and from 0.05 $M_{\rm Jup}$ to 0.1 $M_{\rm Jup}$ at $\alpha = -0.3$ (corresponding to the F values of 0.48 ± 0.34 and 0.15 ± 0.10, respectively). Our detections thus indicate that the mass function lies within these limits, and that the exoplanet mass function at low masses is more likely to be roughly flat $\alpha \sim -1$ rather than steep. Although the constraints from this initial Rocky Planet Search observing run are relatively modest, our simulations offer a direct methodology to determine an empirical exoplanet mass function. These can readily be improved with (1) an expanded sample of high-precision data on a larger sample, (2) simulations covering larger sets of the high-precision AAPS matching the quality obtained in this intensive observing run, (3) higher resolution simulations (i.e., more realizations at more closely sampled orbital parameters), and (4) further improvements in our understanding of stellar jitter and convective granulation.

We thank the anonymous referee for comments and suggestions that helped improve the paper. We acknowledge support from the following grants: NSF AST-9988087, NASA NAG5-12182, PPARC/STFC PP/C000552/1, and ARC Discovery DP774000; and travel support from the Carnegie Institution of Washington and the Anglo-Australian Observatory. This research has made use of NASA's Astrophysics Data System, and the SIMBAD database, operated at CDS, Strasbourg, France. We are extremely grateful for the uniformly excellent and extraordinary support we have received from the AAT's technical staff over the last 10 yr. We also extend our effusive thanks to Professor Matthew Bailes and the staff at the Swinburne Supercomputing Centre for allowing us the use of their facilities, and providing support and assistance when required. The authors acknowledge the use of UCL Research Computing facilities and services in the completion of this work.

Facility: AAT

REFERENCES

Alonso, A., Arribas, S., & Martínez-Roger, C. 1996, A&A, 313, 873
Bailey, J. A., Butler, R. P., Tinney, C. G., Jones, H. R. A., O'Toole, S. J., Carter, B. D., & Marcy, G. W. 2008, ApJ, 690, 743
Beaulieu, J.-P., et al. 2006, Nature, 439, 437
Bennett, D. P., et al. 2008, ApJ, 684, 663
Boss, A. P. 2007, ApJ, 661, L73
Butler, R. P., Marcy, G. W., Williams, E., McCarthy, C., Dosanjh, P., & Vogt, S. S. 1996, PASP, 108, 500
Butler, R. P., Tinney, C. G., Marcy, G. W., Jones, H. R. A., Penny, A. J., & Apps, K. 2001, ApJ, 555, 410
Butler, R. P., et al. 2002, ApJ, 578, 565
Butler, R. P., et al. 2006, ApJ, 646, 505
Carter, B. D., et al. 2003, ApJ, 593, L43
Cumming, A. 2004, MNRAS, 354, 1165
Cumming, A., Butler, R. P., Marcy, G. W., Vogt, S. S., Wright, J. T., & Fischer, D. A. 2008, PASP, 120, 531
Cumming, A., Marcy, G. W., & Butler, R. P. 1999, ApJ, 526, 890
Cumming, A., Marcy, G. W., Butler, R. P., & Vogt, S. S. 2003, in ASP Conf. Ser. 294, Scientific Frontiers in Research on Extrasolar Planets (San Francisco, CA: ASP), 27
Demarque, P., Woo, J.-H., Kim, Y.-C., & Yi, S. K. 2004, ApJS, 155, 667
Diego, F., Charalambous, A., Fish, A. C., & Walker, D. D. 1990, Proc. Soc. Photo-Opt. Instrum. Eng., 1235, 562
Girardi, L., Bressan, A., Bertelli, G., & Chiosi, C. 2000, A&AS, 141, 371
Goldreich, P., Lithwick, Y., & Sari, R. 2004, ApJ, 614, 497
Haisch, K. E., Jr., Lada, E. A., & Lada, C. J. 2001, ApJ, 553, L153
Henry, T. J., Soderblom, D. R., Donahue, R. A., & Baliunas, S. L. 1996, AJ, 111, 439
Hillenbrand, L. A., Strom, S. E., Calvet, N., Merrill, K. M., Gatley, I., Makidon, R. B., Meyer, M. R., & Skrutskie, M. F. 1998, AJ, 116, 1816
Houk, N. 1982, Michigan Catalog of Two Dimensional Spectral Types for the HD Stars, Vol. 3 (Ann Arbor, MI: University of Michigan Press)
Ida, S., & Lin, D. N. C. 2004, ApJ, 604, 388
Jenkins, J. S., et al. 2006, MNRAS, 372, 163
Jones, H. R. A., Butler, R. P., Marcy, G. W., Tinney, C. G., Penny, A. J., McCarthy, C., & Carter, B. D. 2002, MNRAS, 333, 871
Jones, H. R. A., Butler, R. P., Marcy, G. W., Tinney, C. G., Penny, A. J., McCarthy, C., & Carter, B. D. 2003a, MNRAS, 337, 1170
Jones, H. R. A., et al. 2003b, MNRAS, 341, 948
Jones, H. R. A., et al. 2006, MNRAS, 369, 249
Kenyon, S. J., & Bromley, B. C. 2006, AJ, 131, 1837
Léger, A., et al. 2004, Icarus, 169, 499
McCarthy, C., et al. 2004, ApJ, 617, 575
Mamajek, E. E., Meyer, M. R., Hinz, P. M., Hoffmann, W. F., Cohen, M., & Hora, J. L. 2004, ApJ, 612, 496
Marcy, G. W., et al. 2005a, ApJ, 619, 570
Marcy, G. W., Butler, R. P., Fischer, D. A., Vogt, S. S., Wright, J. T., Tinney, C. G., & Jones, H. R. A. 2005b, Prog. Theor. Phys. Suppl., 158, 24
Mayor, M., et al. 2008, A&A, 493, 639
Narayan, R., Cumming, A., & Lin, D. N. C. 2005, ApJ, 620, 1002
Nordström, B., et al. 2004, A&A, 418, 989
O'Toole, S. J., Tinney, C. G., & Jones, H. R. A. 2008, MNRAS, 386, 516
O'Toole, S. J., Tinney, C. G., Jones, H. R. A., Butler, R. P., Marcy, G. W., Carter, B., & Bailey, J. 2009a, ApJ, 697, 1263
O'Toole, S. J., Tinney, C. G., Jones, H. R. A., Butler, R. P., Marcy, G. W., Carter, B., & Bailey, J. 2009b, MNRAS, 392, 641
O'Toole, S., et al. 2007, ApJ, 647, 594
Perryman, M. A. C., et al. 1997, A&A, 323, L49
Pollack, J. B., Hubickyj, O., Bodenheimer, P., Lissauer, J. J., Podolak, M., & Greenzweig, Y. 1996, Icarus, 124, 62
Rivera, E. J., et al. 2005, ApJ, 634, 625
Salasnich, B., Girardi, L., Weiss, A., & Chiosi, C. 2000, A&A, 361, 1023

Shen, Y., & Turner, E. L. 2008, ApJ, 685, 553
Tinney, C. G., Butler, R. P., Marcy, G. W., Jones, H. R. A., Penny, A. J., McCarthy, C., & Carter, B. D. 2002a, ApJ, 571, 528
Tinney, C. G., McCarthy, C., Jones, H. R. A., Butler, R. P., Carter, B. D., Marcy, G. W., & Penny, A. J. 2002b, MNRAS, 332, 759
Tinney, C. G., et al. 2001, ApJ, 551, 507
Tinney, C. G., et al. 2003, ApJ, 587, 423
Tinney, C. G., et al. 2005, ApJ, 623, 1171
Tinney, C. G., et al. 2006, ApJ, 647, 594
Udry, S., et al. 2000, A&A, 356, 590
Udry, S., et al. 2006, A&A, 447, 361
Udry, S., et al. 2007, A&A, 469, L37
Valenti, J. A., Butler, R. P., & Marcy, G. W. 1995, PASP, 107, 966
Valenti, J. A., & Fischer, D. A. 2005, ApJS, 159, 141
Wetherill, G. W., & Stewart, G. R. 1989, Icarus, 77, 330
Wittenmyer, R. A., Endl, M., Cochran, W. D., Hatzes, A. P., Walker, G. A. H., Yang, S. L. S., & Paulson, D. B. 2006, AJ, 132, 177
Wright, J. T. 2005, PASP, 117, 657